

# Not All Denoising Steps Are Equal: Model Scheduling for Faster Masked Diffusion Language Models

Ivan Sedykh<sup>1</sup> Nikita Sorokin<sup>1</sup> Valentin Malykh<sup>1,2</sup>

## Abstract

Recent advances in masked diffusion language models (MDLMs) narrow the quality gap to autoregressive LMs, but their sampling remains expensive because generation requires many full-sequence denoising passes with a large Transformer and, unlike autoregressive decoding, cannot benefit from KV caching. In this work, we exploit the flexibility of the diffusion framework and study model scheduling, where a smaller MDLM replaces the full model at a subset of denoising steps. On OpenWebText, we show that early and late denoising steps are substantially more robust to such replacement than middle steps, enabling up to a 17% reduction in FLOPs with only modest degradation in generative perplexity. We support these findings with a step-importance analysis based on loss and KL divergence between small and large models across timesteps, as well as an exhaustive search over coarse step segments, both of which identify the middle of the diffusion trajectory as most sensitive. Our results suggest that simple, architecture-agnostic scheduling rules can significantly accelerate MDLM sampling while largely preserving generation quality as measured by generative perplexity.

## 1. Introduction

Masked diffusion language models (MDLMs) (Sahoo et al., 2024) have recently emerged as a competitive alternative to autoregressive language models, narrowing the quality gap (Gong et al., 2025; Nie et al., 2025b; Ye et al., 2025a) while offering a different generation paradigm based on iterative denoising. However, MDLM sampling remains expensive: generation requires many full-sequence denoising passes with a large Transformer, and unlike autoregressive decoding, this process cannot benefit from KV caching (Wu

<sup>1</sup>MWS AI <sup>2</sup>ITMO University. Correspondence to: Ivan Sedykh <i.sedykh@mts.ai>.

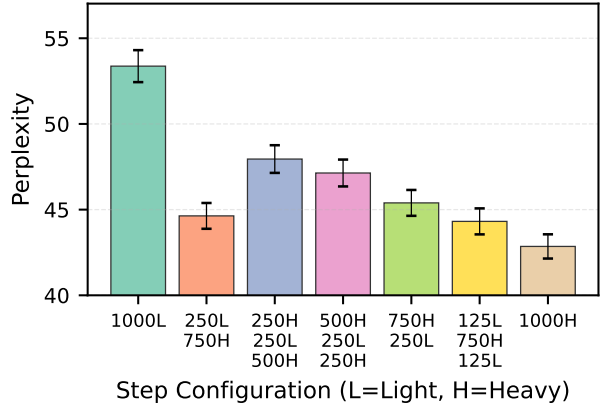


Figure 1. Generative perplexity (GPT-2) for hand-crafted model schedules using a heavy 12-block model and a light 4-block model with exactly 250/1000 light steps (16.7% saved FLOPs). Each bar label encodes a schedule as contiguous segments, e.g., (L125, H750, L125) denotes the *sandwich* schedule (125 light steps, 750 heavy steps, 125 light steps), while placing all light steps in the 2nd or 3rd quarter yields the worst perplexity. Error bars correspond to 95% confidence intervals.

et al., 2025a;b). As a result, even when MDLM quality is strong, inference cost can be a practical bottleneck.

A distinctive feature of diffusion models is that generation proceeds through a sequence of timesteps that gradually transform a high-noise (or heavily corrupted) state into a clean sample. This structure suggests a natural question: are all denoising steps equally “difficult,” and therefore equally deserving of full model capacity? In continuous image diffusion, a growing body of work (Shen et al., 2024; Huang et al., 2025) explores timestep-dependent compute allocation, including approaches that skip, cache, or dynamically adjust capacity across the trajectory. These methods are motivated by evidence that model behavior varies systematically across timesteps, often exhibiting relatively smooth or monotonic trends in step difficulty. For example, DyDiT++ (Zhao et al., 2025) analyzes loss differences between small and large diffusion Transformers and reports that these differences can shrink toward one end of the trajectory, suggesting that some timesteps may be handled effectively by smaller models.

Whether similar conclusions hold for discrete masked diffusion in language remains unclear. Text denoising differs from image denoising in both the state space (discrete tokens with masking) and the structure of the prediction problem (categorical distributions over vocabularies, with uncertainty concentrated on masked positions). Consequently, step-importance patterns and effective acceleration strategies may not transfer directly from continuous image diffusion to masked diffusion for text.

In this work, we study model scheduling for faster MDLM sampling: at inference time, we replace a subset of denoising steps of a large “heavy” MDLM with a separately trained smaller “light” MDLM. This approach is intentionally simple and architecture-agnostic: it does not require retraining the heavy model, distillation, or modifying the sampling algorithm beyond choosing which model to run at each step. The central question is then straightforward: **which timesteps are most robust to model replacement, and how should light and heavy steps be arranged to best trade off speed and quality?**

Our empirical results on OpenWebText show that denoising steps are not equally important for masked diffusion generation. When we fix a compute budget (e.g., replacing 25% of steps with a light model), the placement of these light steps matters substantially: replacing steps in the middle of the trajectory yields the largest degradation in generative perplexity, while allocating light steps near the beginning and end performs best. In particular, a simple sandwich schedule that places light steps at both ends of the trajectory consistently outperforms schedules that concentrate light steps in the middle. These observations enable meaningful inference savings, achieving up to a 17% reduction in FLOPs with only modest degradation in generative perplexity.

To validate that this pattern is not an artifact of a small set of hand-designed schedules, we perform an exhaustive search over coarse step segments and find the same qualitative conclusion: middle segments are the most sensitive to replacement, while the earliest and latest segments are relatively safe. This yields a practical rule of thumb: under a fixed budget of cheap steps, it is preferable to distribute them across both ends of the trajectory rather than concentrating them in the middle.

We further support these findings with a step-importance analysis based on **model similarity vs. timestep**. We compare light and heavy models on the same corrupted inputs at each timestep and measure their disagreement via differences in masked-token cross-entropy and token-level KL divergence. Both measures exhibit a clear peak in the middle of the trajectory, indicating maximal divergence between small and large models at intermediate noise levels. This provides a mechanistic explanation for why middle-step replacement is most harmful and clarifies how step sensitiv-

ity in masked diffusion for text differs from the smoother, often monotonic step-importance trends reported in prior continuous image diffusion analyses.

In summary, our contributions are:

1. Model scheduling for MDLMs: We study an inference-time acceleration strategy that mixes a heavy MDLM with a separately trained light MDLM across denoising steps, without distillation or architecture modification.
2. Empirical step-importance finding: On OpenWebText, we show that early and late denoising steps are substantially more robust to model replacement than middle steps, enabling up to 17% FLOPs reduction with modest perplexity degradation under effective schedules.
3. Explanatory analysis: We provide complementary evidence from (i) loss/KL-based similarity across timesteps and (ii) exhaustive search over coarse segments, both identifying the middle of the trajectory as most compute-sensitive.

Section 2 reviews masked diffusion LMs and related efficiency work; Section 3 introduces model scheduling; Section 4 presents empirical results and step-importance analyses; Section 5 discusses limitations and future directions.

## 2. Related Work

### 2.1. Diffusion Models

Denoising diffusion probabilistic models (DDPMs) (Ho et al., 2020) and score-based generative models (Song et al., 2021) have become a standard framework for high-fidelity generation. Beyond the original ancestral samplers, a large body of work has improved sampling efficiency via alternative discretizations and solvers (Song et al., 2022; Lu et al., 2022). For high-capacity backbones, diffusion transformers (DiT) (Peebles & Xie, 2023) and related Transformer-based score/denoiser parameterizations dominate modern image diffusion systems (Rombach et al., 2022).

### 2.2. Combining Diffusion Models

A classical way to combine models at sampling time is guidance, including classifier guidance (Dhariwal & Nichol, 2021) and classifier-free guidance (CFG) (Ho & Salimans, 2022). Closer to our setting, several vision works explicitly mix models of different sizes across the denoising trajectory to trade off speed and quality without retraining: OMS-DPM (Liu et al., 2023) searches for an optimal per-timestep model assignment under a time budget, while T-Stitch (Pan et al., 2023) “stitches” a small model into the early part of the trajectory as a drop-in replacement.

### 2.3. Diffusion Models Acceleration

Diffusion acceleration methods fall into two broad categories: reducing the number of function evaluations (e.g., DDIM (Song et al., 2021), DPM-Solver (Lu et al., 2022)) and reducing the cost of each evaluation (distillation/consistency and architecture-level adaptivity). Distillation-based methods such as progressive distillation (Salimans & Ho, 2022) and consistency models (Song et al., 2023) aim to preserve quality with fewer steps. A complementary direction makes the *denoiser itself* compute-adaptive. Step-aware or schedule-aware diffusion backbones include DDSM (Yang et al., 2024), which studies step importance and step-dependent capacity, as well as diffusion-transformer specific techniques that skip/caches computation or dynamically route capacity, such as Learning-to-Cache (Ma et al., 2024), Dynamic Diffusion Transformers (DyDiT) (Zhao et al., 2025), MD-DiT (Shen et al., 2024), AdaDiff (Tang et al., 2024). Related NAS-style methods (e.g., Flexiffusion (Huang et al., 2025)) also optimize which segments are full/cached/skipped to meet a compute target. These works are primarily developed and evaluated in continuous image diffusion, and their conclusions about which timesteps deserve more capacity do not necessarily transfer to discrete masked diffusion for text.

### 2.4. Masked Diffusion Language Models

Diffusion for text has been explored in both continuous and discrete spaces. Continuous-text diffusion includes Diffusion-LM (Li et al., 2022), latent variants (Lovelace et al., 2023), and conditional variants such as DiffuSeq (Gong et al., 2023) and simplex-based (Meshchaninov et al., 2025; Shabalin et al., 2025). Discrete diffusion models for language build on discrete-state diffusion formulations such as D3PM (Austin et al., 2023), and include Diffusion-BERT (He et al., 2022) and Score Entropy Discrete Diffusion (SEDD) (Lou et al., 2024). Recent masked diffusion language models (MDLMs) (Sahoo et al., 2024; Shi et al., 2025) show that a simple masked diffusion objective with strong training recipes can close much of the quality gap to autoregressive LMs, and ReMDM (Wang et al., 2025) improves sampling via inference-time remasking and compute scaling. Compared to AR LMs, diffusion LMs can also be stronger learners under data-constrained settings (Ni et al., 2025; Rütte et al., 2025).

Several efforts scale diffusion LMs and explore hybridization with autoregressive decoding, including large-scale MDLM reports such as LLaDA (Nie et al., 2025b) and Dream (Ye et al., 2025a), as well as domain/architecture variants such as DiffuCoder (Gong et al., 2025) and Dif-LLaMA (Nie et al., 2025a). A separate line of work targets inference efficiency. Some methods recover or ap-

proximate KV-cache benefits for bidirectional diffusion via block/hybrid formulations and cache reuse (Arriola et al., 2025a; Wu et al., 2025a; Sahoo et al., 2025; Arriola et al., 2025b; Wu et al., 2025b). Others reduce the effective number of denoising iterations through adaptive or distilled decoding policies, including FlashDLM (FreeCache and AR-guided step reduction) (Hu et al., 2025), LocalLeap (Kong et al., 2025), and CD4LM (Liang et al., 2026). Finally, dInfer provides a system-oriented framework with modular decoding strategies and KV-cache management for efficient diffusion-LM serving (Ma et al., 2025). These approaches are largely *orthogonal* to our model scheduling: they reduce the number of denoising iterations, the per-step attention cost via caching, and/or system overhead, whereas we vary *model capacity across steps* without modifying the sampler. In principle, scheduling composes with KV caching (apply caching within both heavy and light steps) and with step-reduction decoders (apply capacity scheduling within the remaining iterations), suggesting multiplicative speedups.

Finally, token difficulty is known to be non-uniform in autoregressive generation, with evidence that per-position perplexity can vary systematically across a sequence (Helm et al., 2025; Zur et al., 2025; Yang & Holtzman, 2025; Bell et al., 2025); this motivates exploring whether “where to spend compute” is similarly non-uniform across diffusion timesteps in masked diffusion generation.

## 3. Accelerating MDLM via Model Scheduling

### 3.1. Experimental setup

**Masked diffusion language models.** Let  $x = (x^{(1)}, \dots, x^{(L)})$  denote a clean (denoised) token sequence of length  $L$ . Autoregressive language models generate  $x$  sequentially by modeling  $p_\theta(x^{(i)} | x^{(<i>})})$  and are typically trained with a token-level cross-entropy objective. In contrast, masked diffusion language models (MDLMs) generate text by repeatedly denoising a partially masked sequence. Concretely, we define a discrete forward noising process  $q$  that corrupts  $x$  into  $z_t$  by replacing tokens with a special mask token  $m$  according to a time-dependent corruption level.

**Forward process  $q(z_t | x)$ .** We represent each token as a one-hot vector in  $\{0, 1\}^{|V|}$ . For a normalized time  $t \in [0, 1]$ , the forward process produces a noisy sequence  $z_t = (z_t^{(1)}, \dots, z_t^{(L)})$  with independent per-position marginals

$$q(z_t^{(\ell)} | x^{(\ell)}) = \text{Cat}(\alpha_t x^{(\ell)} + (1 - \alpha_t) \pi), \quad (1)$$

where  $\pi$  is a fixed prior distribution over vocabulary symbols. In our setting we use *pure masking*, i.e.,  $\pi = \delta_m$ , so that with probability  $(1 - \alpha_t)$  a token is replaced by  $m$ , and otherwise it is kept unchanged. We use a *linear* schedule

$\alpha_t = 1 - t$ , so that the expected masked fraction equals  $t$ . During training we sample  $t \sim \mathcal{U}(0, 1)$ .

Let  $M(z_t) \subseteq \{1, \dots, L\}$  denote the set of masked positions in  $z_t$ , i.e.,  $M(z_t) = \{\ell : z_t^{(\ell)} = m\}$ .

**Denoiser and training objective.** The denoiser  $p_\theta(x | z_t, t)$  is parameterized by a bidirectional Transformer that predicts the original token at each position given the noisy sequence and timestep. Training minimizes a weighted masked language modeling loss over masked positions only. Following prior derivations of the (negative) ELBO for this discrete diffusion process, the objective can be written as

$$\begin{aligned} \mathcal{L}_{\text{MDLM}}(x) &= \mathbb{E}_{t \sim \mathcal{U}(0,1), z_t \sim q(\cdot|x)} [\ell_\theta(x; z_t, t)], \\ \ell_\theta(x; z_t, t) &= \frac{\alpha'_t}{1 - \alpha_t} \sum_{\ell \in M(z_t)} -\log p_\theta(x^{(\ell)} | z_t, t). \end{aligned} \quad (2)$$

Here  $\alpha'_t$  denotes the derivative of  $\alpha_t$  with respect to  $t$ . The factor  $\frac{\alpha'_t}{1 - \alpha_t}$  reweights timesteps so that different corruption levels contribute appropriately to the variational objective; for  $\alpha_t = 1 - t$ , we have  $\frac{-\alpha'_t}{1 - \alpha_t} = \frac{1}{t}$ .

**Sampling (reverse process).** To generate an unconditional sequence of length  $L$ , sampling starts from a fully masked sequence  $z_{t=1}$  where  $z_{t=1}^{(\ell)} = m$  for all  $\ell$ . The reverse process proceeds for  $T$  discrete steps with times  $t_i = i/T$  for  $i = T, T - 1, \dots, 0$ . We use the standard MDLM sampler (no remasking): once a token is generated (unmasked), it remains fixed thereafter. Multiple tokens can be updated in parallel at each step (unlike autoregressive decoding); however, each denoising step requires a full bidirectional Transformer forward pass over the entire sequence, and thus inference cost scales with the number of denoising evaluations.

**Why sampling is expensive.** Although MDLM sampling updates many tokens at once, it typically requires a large number of sequential denoising steps and does not admit the KV-caching efficiency of autoregressive decoding. This motivates our focus on *model scheduling*: replacing the full denoiser with a smaller denoiser on a subset of timesteps to reduce total compute while retaining generation quality.

**Model scheduling.** Let  $\{\theta_k\}_{k \in \mathcal{K}}$  denote a set of denoisers of different sizes (e.g.,  $k \in \{4, 6, 8, 10, 12\}$  Transformer blocks) trained with the same objective and noise schedule. A *model schedule* is a function  $s : \{1, \dots, T\} \rightarrow \mathcal{K}$  that selects which denoiser to use at each reverse step  $i$  (time  $t_i = i/T$ ). Sampling then applies  $p_{\theta_{s(i)}}(\cdot | z_{t_i}, t_i)$  at step  $i$ . If the heavy model has  $B_H = 12$  blocks and the light model has  $B_L$  blocks, then replacing a fraction  $p$  of steps by the

light model yields a relative compute reduction of

$$\text{saved FLOPs} \approx p \cdot \frac{B_H - B_L}{B_H}. \quad (3)$$

**Models and training details.** To avoid confounding factors and isolate the effect of scheduling, we closely follow the MDLM training setup (Sahoo et al., 2024) and use their codebase and default design choices whenever possible. We train a family of Transformer-encoder denoisers (Vaswani et al., 2017; Devlin et al., 2019) that differ *only* in depth (4/6/8/10/12 blocks) while keeping width fixed (hidden size 768, MLP ratio 4, same vocabulary/tokenizer). The 12-block model serves as the *heavy* baseline, and the smaller models serve as candidate *light* denoisers. Because Transformer blocks are executed sequentially, both runtime and FLOPs scale approximately linearly with the number of blocks, enabling simple and reliable compute accounting for our schedules.

All models are trained on OpenWebText (Gokaslan et al., 2019) tokenized with the GPT-2 tokenizer (Brown et al., 2020) for 1M optimization steps with effective batch size 512 and sequence length 1024. This corresponds to approximately 262B masked tokens during training. We choose OpenWebText as a broad, general-purpose natural language corpus to study unconditional generation and isolate the effect of timestep scheduling without task-specific structure. We use AdamW (Loshchilov & Hutter, 2017) with 2500 linear warmup steps, learning rate  $3 \cdot 10^{-4}$ , and  $\beta = (0.9, 0.999)$  (other hyperparameters follow (Sahoo et al., 2024)).

**Evaluation metric.** To measure unconditional generation quality, we follow MDLM (Sahoo et al., 2024) and report *generative perplexity* computed by a pretrained GPT-2 (Brown et al., 2020) model on fully unconditional samples. Unless stated otherwise, we generate 1600 independent samples of length 1024 using  $T = 1000$  denoising steps and compute mean perplexity. We acknowledge that generative perplexity can be unreliable in some settings (e.g., ReMDM (Wang et al., 2025) discusses failure modes), but in this work we compare schedules under identical training and sampling protocols, and use it as a consistent *relative* metric across configurations.

### 3.2. Fixed light-step ratio (25%)

We first consider a simple setting with two models: a 12-block heavy MDLM and a 4-block light MDLM. We replace exactly 25% of the heavy model’s denoising steps with the light model and ask: *which steps should be replaced to minimize quality loss?* Under our compute accounting 3, the saved FLOPs are 16.7%. Although our framework naturally extends to using more than two models, we focus on

this clear two-model setup to make the effect of schedule placement easy to interpret.

We test several hand-crafted schedules that place the 250 light steps in different parts of the trajectory (by quarters), and also a *sandwich* schedule that splits the 250 light steps into two equal segments of 125 and places them at the beginning and end of the trajectory. The results are shown in Figure 9. Replacing steps in the middle of the trajectory (2nd/3rd quarters) yields the worst perplexity, while the sandwich schedule performs best, closely followed by placing all light steps in the first quarter. These results indicate that denoising steps are not equally important for masked diffusion generation. Additional hand-crafted schedules for other light model sizes are reported in Appendix A and exhibit the same qualitative pattern.

### 3.3. Exhaustive search over coarse step segments

To further validate the above trend under a stronger compute reduction, we replace 400 out of 1000 denoising steps (40%) with the 4-block light model. This corresponds to 26.7% saved FLOPs. While some prior works search over timesteps via learned predictors (Liu et al., 2023) or heuristic optimization schemes (Yang et al., 2024), we perform an exhaustive search in a discretized space for transparency.

A naive search over all subsets of 400 steps is infeasible:  $\binom{1000}{400} \approx 5 \times 10^{290}$ . We therefore partition the 1000 steps into 10 contiguous segments of 100 steps and select 4 segments to run with the light model, resulting in  $\binom{10}{4} = 210$  schedules. For this brute-force experiment, we evaluate each schedule using 160 unconditional samples (fixed seeds across schedules) for tractability.

Figure 2 compares the top-5 and bottom-5 schedules. The best schedules consistently place light segments near the beginning and end of the trajectory, while the worst schedules place light segments predominantly in the middle. We quantify this by counting segment frequency among the top-20 and bottom-20 schedules (Figures 3 and 4). Middle segments appear disproportionately often in the worst schedules, confirming that mid-trajectory steps are the most sensitive to replacement.

**Implementation note.** This coarse segmentation is also convenient in practice: the MDLM sampler can include “no-op” iterations where the mask set does not change, allowing us to reuse logits instead of re-running the Transformer. Using contiguous segments simplifies this bookkeeping (this is not autoregressive KV caching).

As a practical rule of thumb suggested by both the hand-crafted and exhaustive results, spreading cheaper steps across *both* ends of the trajectory tends to be preferable to concentrating them in the middle. For example, for

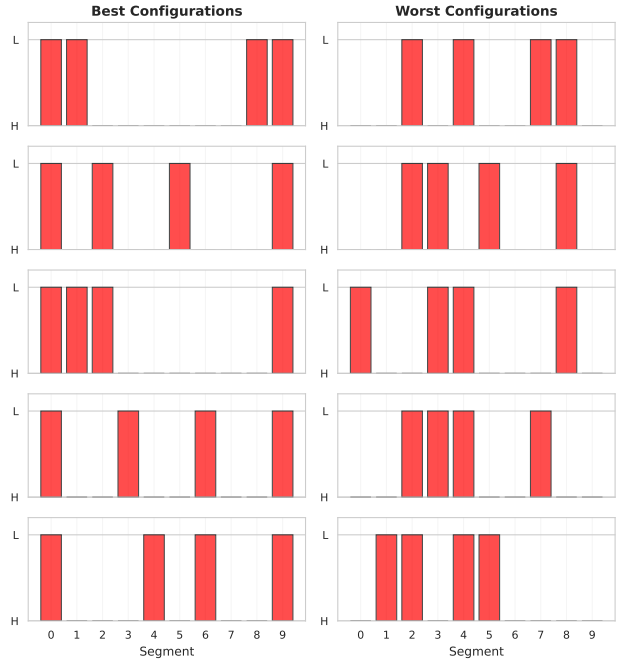


Figure 2. Comparison of the top 5 best (left) and worst (right) model scheduling configurations among the 210 coarse schedules. Each row shows one configuration. Red bars indicate light (4-block) model placement. Segments 0–9 correspond to steps 0–100, 100–200, ..., 900–1000, where segment 0 is closest to the fully masked state ( $t \approx 1$ ). Best configurations concentrate light segments near both ends, while worst configurations place light segments in the middle.

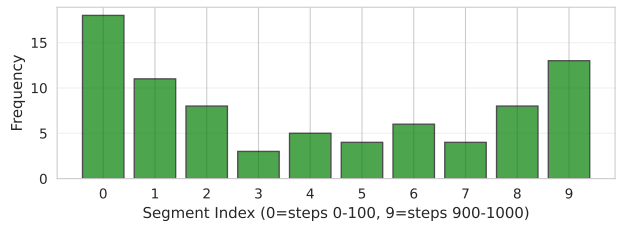


Figure 3. Segment frequency in the top 20 best-performing configurations (lowest perplexity). Bars show how often each segment is assigned to the light (4-block) model across the top-20 schedules. Higher frequency suggests that replacing this segment is relatively safe.

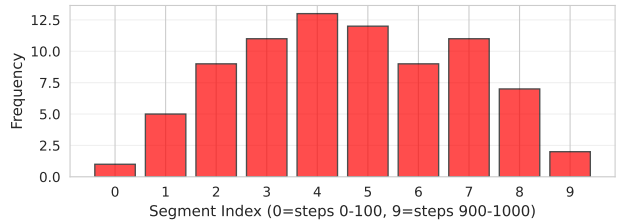


Figure 4. Segment frequency in the bottom 20 worst-performing configurations (highest perplexity). Bars show how often each segment is assigned to the light (4-block) model across the bottom-20 schedules. Higher frequency suggests that replacing this segment is harmful.

600 light steps one can use a symmetric schedule of (L300, H400, L300).

### 3.4. Scaling over light model size / light-step fraction

We next study two scaling dimensions: (i) the size of the light model and (ii) the fraction of light steps. Table 1 fixes the *sandwich* placement (125 light + 750 heavy + 125 light) and varies the light model depth from 4 to 10 blocks, paired with the 12-block heavy baseline. As expected, increasing light-model depth reduces the quality drop while also reducing the achievable FLOPs savings.

Table 2 fixes the model pair (12-block heavy, 4-block light) and varies the percentage of steps executed by the light model from 0% to 100%. In addition to FLOPs-based estimates, we report end-to-end wall-clock time for the same sampling setup. We observe a smooth transition in perplexity as the schedule shifts from fully heavy to fully light, indicating that model scheduling provides a continuous speed-quality tradeoff.

Table 1. Scaling the *light model* while keeping schedule placement fixed to the sandwich pattern (125 light + 750 heavy + 125 light, i.e., 25% light steps). “PPL drop” is relative to the all-heavy 12-block baseline. “Saved FLOPs” is computed as  $0.25 \cdot (12 - B_L)/12$ . Numbers in scriptsize represent 95% confidence intervals.

light model	gen. PPL	PPL drop	saved FLOPs
4b	44.31 ± 0.76	3.41%	16.67%
6b	43.67 ± 0.67	1.94%	12.50%
8b	43.45 ± 0.73	1.40%	8.33%
10b	42.90 ± 0.70	0.12%	4.17%
12b	42.85 ± 0.71	0.00%	0.00%

**Wall-clock vs. FLOPs.** Although our compute estimates scale linearly with Transformer depth, measured wall-clock speedups (Table 2) can deviate because not all inference cost is depth-dependent. In our MDLM implementation, the input/output embedding and, in particular, the final vocabulary projection dominate runtime for smaller models, and these layers are identical across the heavy and light variants. Profiling confirms this effect: for the 4-block model, the output layer accounts for the majority of runtime ( $\approx 81.6\%$ ), whereas the Transformer blocks contribute only  $\approx 18.2\%$ ; for the 12-block model, the output layer remains substantial ( $\approx 59.9\%$ ) while blocks account for  $\approx 40.0\%$ . As a result, reducing depth primarily affects the block compute and yields smaller end-to-end speedups than predicted by FLOPs alone. This mismatch is expected to diminish at larger scales and/or in regimes where block compute dominates (e.g., larger hidden sizes, longer sequences, or architectures where the output projection is relatively less significant). Therefore, FLOPs savings should be interpreted as an upper bound on realized wall-clock gains unless the non-depth-

Table 2. Scaling the *fraction of light steps* for the (12-block heavy, 4-block light) model pair under a ‘sandwich’ pattern.

% light steps	gen. PPL	saved FLOPs	time (s)	speedup
0	42.9	0.0%	109.7	0.0%
10	43.1	6.7%	106.4	3.0%
20	43.8	13.3%	103.3	5.8%
30	44.7	20.0%	100.4	8.5%
40	45.9	26.7%	97.3	11.3%
50	47.2	33.3%	94.3	14.0%
60	48.6	40.0%	91.1	17.0%
70	50.1	46.7%	90.7	17.3%
80	51.4	53.3%	85.4	22.2%
90	52.5	60.0%	84.8	22.7%
100	53.4	66.7%	78.7	28.3%

dependent components (e.g., vocabulary projection and softmax/sampling) are also optimized. Importantly, this bottleneck is not fundamental: more efficient CUDA/Triton implementations for the output projection and softmax/sampling exist (e.g., fused projection-softmax/loss operators as in Liger-Kernel (Hsu et al., 2025), and highly optimized inference kernels in serving stacks such as NVIDIA TensorRT-LLM (NVIDIA, 2026) and FlashInfer (Ye et al., 2025b)). Leveraging such kernels is orthogonal to our scheduling method and can both increase the absolute speedups and bring wall-clock gains closer to FLOPs-based predictions.

**A simple model.** If the end-to-end runtime decomposes as  $T \approx T_{\text{out}} + T_{\text{blocks}}$ , and only  $T_{\text{blocks}}$  scales with depth, then the attainable speedup from reducing depth is limited by the fraction of time spent outside the blocks. Writing  $\alpha := T_{\text{out}}/T$ , the maximum possible speedup satisfies

$$\text{speedup} \leq \frac{1}{1 - \alpha}. \tag{4}$$

## 4. Why does this work? Step importance analysis

### 4.1. Model similarity vs timestep

Inspired by OMS-DPM (Liu et al., 2023), we compare model behavior across noise levels. Following the similarity analyses used in dynamic diffusion transformer works (e.g., (Zhao et al., 2025)), we compute loss differences and KL divergences between models at fixed timesteps. For each timestep we evaluate on 500 sequences of length 1024, and crucially compare models on the *same* corrupted inputs.

**Loss difference.** For a fixed timestep  $t$ , we sample  $z_t \sim q(\cdot | x)$  and compute the (unweighted) masked-token cross-

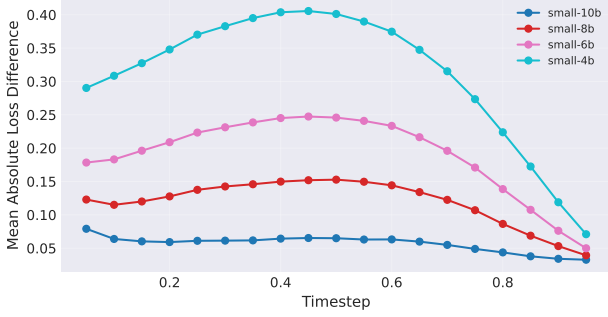


Figure 5. Mean absolute difference in masked-token cross-entropy between each light model and the heavy 12-block baseline across timesteps. Each curve compares one light model to the baseline, evaluated on the same corrupted inputs  $z_t$ . Lower values indicate higher similarity.

entropy

$$\mathcal{L}_\theta(z_t, t) = \frac{1}{|M(z_t)|} \sum_{\ell \in M(z_t)} -\log p_\theta(x^{(\ell)} | z_t, t). \quad (5)$$

We then measure the mean absolute loss difference between a light model  $\theta_L$  and the heavy model  $\theta_H$ :

$$\Delta_{\text{loss}}(t) = \mathbb{E}_x \mathbb{E}_{z_t \sim q(\cdot|x)} |\mathcal{L}_{\theta_L}(z_t, t) - \mathcal{L}_{\theta_H}(z_t, t)|. \quad (6)$$

The result is presented in Figure 5. Prior work on continuous image diffusion often reports a monotonic trend across timesteps (Pan et al., 2024; Zhao et al., 2025). In contrast, we observe a clear peak in the middle of the trajectory, indicating maximal disagreement between light and heavy models at intermediate noise levels.

**KL divergence.** We additionally compare the *token distributions* predicted at masked positions. Let  $p_\theta(\cdot | z_t, t, \ell)$  denote the categorical distribution over the vocabulary for position  $\ell \in M(z_t)$ . We compute the average token-level KL divergence between two models:

$$\Delta_{\text{KL}}(t) = \mathbb{E}_x \mathbb{E}_{z_t \sim q(\cdot|x)} \left[ \frac{1}{|M(z_t)|} \times \sum_{\ell \in M(z_t)} \text{KL}(p_{\theta_H}(\cdot | z_t, t, \ell) \| p_{\theta_L}(\cdot | z_t, t, \ell)) \right]. \quad (7)$$

To account for intrinsic ambiguity in text prediction, we compute a baseline  $\Delta_{\text{KL}}^{\text{base}}(t)$  as the KL divergence between two independently trained heavy (12-block) checkpoints with different random seeds (different initialization and data order), and report the *relative* divergence  $\Delta_{\text{KL}}(t) - \Delta_{\text{KL}}^{\text{base}}(t)$ . Figure 6 shows the same qualitative pattern as Figure 5: disagreement peaks near the middle ( $t \approx 0.4$ – $0.6$ ) and is substantially smaller at both ends. Here  $t = 1$  corresponds to the fully masked state (start of sampling), and  $t \rightarrow 0$  corresponds to the nearly unmasked state (end of sampling).

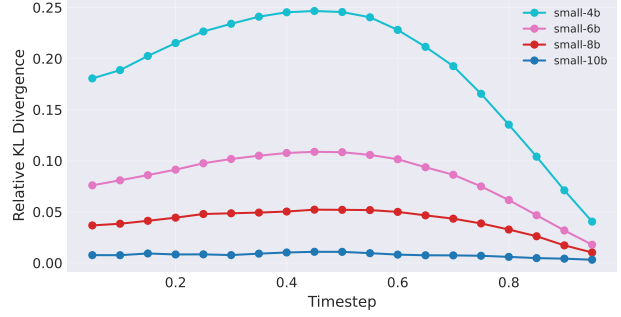


Figure 6. Relative token-level KL divergence (Eq. 7) between model pairs across timesteps, after subtracting a baseline KL curve computed between two independently trained heavy (12-block) checkpoints. Lower values indicate closer agreement. Divergence peaks in the middle of the trajectory, suggesting that intermediate timesteps are most sensitive to model replacement.

## 4.2. Segment influence from exhaustive search

The exhaustive 10-segment search in Section 3.3 provides another way to estimate step importance. For each segment  $j \in \{0, \dots, 9\}$ , let  $\mathcal{S}_j$  be the set of schedules in which segment  $j$  uses the light model, and let  $\text{PPL}(s)$  be the generative perplexity of schedule  $s$ . We compute the segment score as

$$I(j) = \frac{1}{|\mathcal{S}_j|} \sum_{s \in \mathcal{S}_j} \text{PPL}(s) - \frac{1}{|\mathcal{S}|} \sum_{s \in \mathcal{S}} \text{PPL}(s), \quad (8)$$

i.e., the mean perplexity of schedules that use the light model in segment  $j$ , mean-subtracted by the average perplexity over all 210 schedules. Figure 7 shows that middle segments have positive scores (worse than average when replaced), while the earliest and latest segments tend to have negative scores (more robust to replacement). This empirically matches the similarity analysis above and supports the conclusion that intermediate denoising steps are the most compute-sensitive for masked diffusion generation.

## 5. Conclusion

Masked diffusion language models offer a compelling alternative to autoregressive generation, but their practicality is often constrained by expensive sampling that requires many full-sequence denoising passes. In this work we studied model scheduling for masked diffusion LMs: replacing a subset of denoising steps of a heavy model with a separately trained lighter Transformer at inference time. Our results show that timestep importance in masked diffusion for text is strongly non-uniform: intermediate timesteps are the most sensitive to model replacement, while early and late steps are comparatively robust. This enables simple schedules, such as sandwich-style allocation of light steps to the ends of the trajectory, to reduce sampling compute (up to 17% estimated FLOPs in our setting) with only modest degrada-

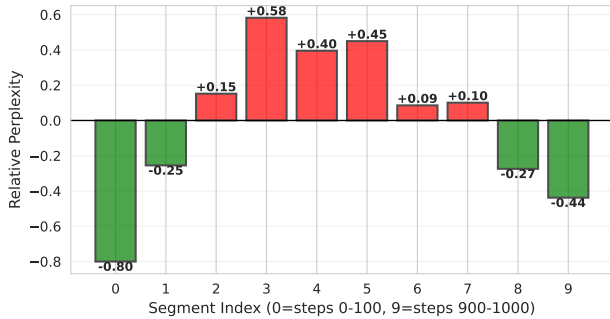


Figure 7. Mean-subtracted segment influence from the exhaustive 10-segment search (Section 3.3). For each segment  $j$ , we compute the mean perplexity over schedules that assign segment  $j$  to the light model, and subtract the mean perplexity over all schedules. Positive values indicate that replacing this segment is harmful on average; negative values indicate that replacing this segment is relatively safe.

tion in generative perplexity. Notably, this pattern contrasts with common observations in image diffusion, where later denoising steps are often reported as more replaceable.

Several natural extensions follow. Currently, pre-trained families of MLMDs spanning multiple scales are not yet standard in the way they are for autoregressive LMs (e.g., Qwen (Yang et al., 2025) or LLaMA (Touvron et al., 2023)). When such families become available, it will be important to verify our claims at larger scale using established benchmarks. Second, scheduling can be generalized beyond two models by using more than two capacity levels during denoising. Finally, rather than fixed schedules, dynamic computation mechanisms such as early-exit strategies or routing policies that adapt compute to the current denoising state may further improve the speed-quality tradeoff.

We hope this work encourages more systematic study of timestep-dependent compute allocation for discrete diffusion language modeling and helps make masked diffusion LMs more efficient at inference time.

## Impact Statement

This paper proposes an inference-time efficiency method for masked diffusion language models by scheduling denoising steps across models of different sizes. The primary intended impact is to reduce sampling computation, which can lower energy use, monetary cost, and associated carbon emissions from running and evaluating generative models. Improved efficiency can also broaden accessibility for researchers and practitioners with limited compute budgets, and may reduce concentration of advanced generative modeling work within a small number of well-resourced organizations.

These potential benefits have environmental and distributive dimensions. Large-scale model training and inference con-

sume substantial electricity; lowering per-sample compute can reduce the footprint of experimentation and deployment and, depending on the energy mix, reduce greenhouse gas emissions. To the extent that compute and energy costs are passed on to communities through higher energy demand and pollution externalities, efficiency improvements can contribute (at the margin) to mitigating those burdens. However, the net environmental impact is ambiguous: efficiency gains can also lead to increased overall usage (a rebound effect), potentially offsetting per-sample savings if deployment scales up.

At the same time, making text generation cheaper and easier to deploy can amplify existing misuse risks associated with generative language models, including spam, phishing, misinformation, and other forms of automated manipulation, by increasing the feasible volume of generated content. This work does not introduce new model capabilities beyond what is already present in the underlying models; it primarily changes how computation is allocated during sampling. Nevertheless, we recommend that any deployment of models benefiting from these efficiency improvements follows standard responsible-use practices, such as access controls, abuse monitoring, rate limiting, and content safety filtering, and that evaluations consider both performance and environmental implications (e.g., reporting compute and energy metrics alongside quality).

## References

- Arriola, M., Gokaslan, A., Chiu, J. T., Yang, Z., Qi, Z., Han, J., Sahoo, S. S., and Kuleshov, V. Block Diffusion: Interpolating Between Autoregressive and Diffusion Language Models, May 2025a. URL <http://arxiv.org/abs/2503.09573>. arXiv:2503.09573 [cs].
- Arriola, M., Schiff, Y., Phung, H., Gokaslan, A., and Kuleshov, V. Encoder-Decoder Diffusion Language Models for Efficient Training and Inference, October 2025b. URL <https://arxiv.org/abs/2510.22852v1>.
- Austin, J., Johnson, D. D., Ho, J., Tarlow, D., and Berg, R. v. d. Structured Denoising Diffusion Models in Discrete State-Spaces, February 2023. URL <http://arxiv.org/abs/2107.03006>. arXiv:2107.03006 [cs].
- Bell, T., Mudireddy, A., Johnson-Eversoll, I., Dasgupta, S., and Mudumbai, R. Slaves to the Law of Large Numbers: An Asymptotic Equipartition Property for Perplexity in Generative Language Models, September 2025. URL <http://arxiv.org/abs/2405.13798>. arXiv:2405.13798 [cs].
- Brown, T. B., Mann, B., Ryder, N., Subbiah, M., Kaplan, J., Dhariwal, P., Neelakantan, A., Shyam, P., Sastry, G.,

- Askill, A., Agarwal, S., Herbert-Voss, A., Krueger, G., Henighan, T., Child, R., Ramesh, A., Ziegler, D. M., Wu, J., Winter, C., Hesse, C., Chen, M., Sigler, E., Litwin, M., Gray, S., Chess, B., Clark, J., Berner, C., McCandlish, S., Radford, A., Sutskever, I., and Amodei, D. Language models are few-shot learners. *arXiv preprint arXiv:2005.14165*, 2020.
- Devlin, J., Chang, M., Lee, K., and Toutanova, K. BERT: pre-training of deep bidirectional transformers for language understanding. In Burstein, J., Doran, C., and Solorio, T. (eds.), *Proceedings of the 2019 Conference of the North American Chapter of the Association for Computational Linguistics: Human Language Technologies, NAACL-HLT 2019, Minneapolis, MN, USA, June 2-7, 2019, Volume 1 (Long and Short Papers)*, pp. 4171–4186. Association for Computational Linguistics, 2019. doi: 10.18653/V1/N19-1423. URL <https://doi.org/10.18653/v1/n19-1423>.
- Dhariwal, P. and Nichol, A. Diffusion Models Beat GANs on Image Synthesis, June 2021. URL <http://arxiv.org/abs/2105.05233>. arXiv:2105.05233 [cs].
- Gokaslan, A., Cohen, V., Pavlick, E., and Tellex, S. Openwebtext corpus. <http://SkyLion007.github.io/OpenWebTextCorpus>, 2019.
- Gong, S., Li, M., Feng, J., Wu, Z., and Kong, L. DiffuSeq: Sequence to Sequence Text Generation with Diffusion Models, February 2023. URL <http://arxiv.org/abs/2210.08933>. arXiv:2210.08933 [cs].
- Gong, S., Zhang, R., Zheng, H., Gu, J., Jaitly, N., Kong, L., and Zhang, Y. DiffuCoder: Understanding and Improving Masked Diffusion Models for Code Generation, June 2025. URL <http://arxiv.org/abs/2506.20639>. arXiv:2506.20639 [cs].
- He, Z., Sun, T., Wang, K., Huang, X., and Qiu, X. Diffusion-BERT: Improving Generative Masked Language Models with Diffusion Models, November 2022. URL <http://arxiv.org/abs/2211.15029>. arXiv:2211.15029 [cs] version: 2.
- Helm, F., Daheim, N., and Gurevych, I. Token Weighting for Long-Range Language Modeling, March 2025. URL <http://arxiv.org/abs/2503.09202>. arXiv:2503.09202 [cs] version: 1.
- Ho, J. and Salimans, T. Classifier-Free Diffusion Guidance, July 2022. URL <http://arxiv.org/abs/2207.12598>. arXiv:2207.12598 [cs].
- Ho, J., Jain, A., and Abbeel, P. Denoising Diffusion Probabilistic Models, December 2020. URL <http://arxiv.org/abs/2006.11239>. arXiv:2006.11239 [cs].
- Hsu, P.-L., Dai, Y., Kothapalli, V., Song, Q., Tang, S., Zhu, S., Shimizu, S., Sahni, S., Ning, H., Chen, Y., and Wang, Z. Liger-kernel: Efficient triton kernels for LLM training. In *Championing Open-source Development in ML Workshop @ ICML25*, 2025. URL <https://openreview.net/forum?id=36SjAIT42G>.
- Hu, Z., Meng, J., Akhauri, Y., Abdelfattah, M. S., sun Seo, J., Zhang, Z., and Gupta, U. Flashdlm: Accelerating diffusion language model inference via efficient kv caching and guided diffusion. *arXiv preprint arXiv:2505.21467*, 2025.
- Huang, H., Chang, X., and Yao, L. Flexiffusion: Segment-wise Neural Architecture Search for Flexible Denoising Schedule, June 2025. URL <http://arxiv.org/abs/2409.17566>. arXiv:2409.17566 [cs].
- Kong, F., Zhang, J., Liu, Y., Wu, Z., Tian, Y., W., V., and Zhou, G. Accelerating diffusion llm inference via local determinism propagation. *arXiv preprint arXiv:2510.07081*, 2025.
- Li, X. L., Thickstun, J., Gulrajani, I., Liang, P., and Hashimoto, T. B. Diffusion-lm improves controllable text generation. In Koyejo, S., Mohamed, S., Agarwal, A., Belgrave, D., Cho, K., and Oh, A. (eds.), *Advances in Neural Information Processing Systems 35: Annual Conference on Neural Information Processing Systems 2022, NeurIPS 2022, New Orleans, LA, USA, November 28 - December 9, 2022*, 2022. URL [http://papers.nips.cc/paper\\_files/paper/2022/hash/1be5bc25d50895ee656b8c2d9eb89d6a-Abstract-Conference.html](http://papers.nips.cc/paper_files/paper/2022/hash/1be5bc25d50895ee656b8c2d9eb89d6a-Abstract-Conference.html).
- Liang, Y., Wang, Z., Chen, H., Sun, X., Wu, J., Yu, X., Liu, J., Barsoum, E., Liu, Z., and Jha, N. K. Cd4lm: Consistency distillation and adaptive decoding for diffusion language models. *arXiv preprint arXiv:2601.02236*, 2026.
- Liu, E., Ning, X., Lin, Z., Yang, H., and Wang, Y. OMS-DPM: Optimizing the Model Schedule for Diffusion Probabilistic Models. In *Proceedings of the 40th International Conference on Machine Learning*, pp. 21915–21936. PMLR, July 2023. URL <https://proceedings.mlr.press/v202/liu23ab.html>.
- Loshchilov, I. and Hutter, F. Decoupled weight decay regularization. *arXiv preprint arXiv:1711.05101*, 2017.
- Lou, A., Meng, C., and Ermon, S. Discrete Diffusion Modeling by Estimating the Ratios of the Data Distribution, June 2024. URL <http://arxiv.org/abs/2310.16834>. arXiv:2310.16834 [stat].

- Lovelace, J., Kishore, V., Wan, C., Shekhtman, E., and Weinberger, K. Q. Latent Diffusion for Language Generation, November 2023. URL <http://arxiv.org/abs/2212.09462>. arXiv:2212.09462 [cs].
- Lu, C., Zhou, Y., Bao, F., Chen, J., Li, C., and Zhu, J. DPM-Solver: A Fast ODE Solver for Diffusion Probabilistic Model Sampling in Around 10 Steps, October 2022. URL <http://arxiv.org/abs/2206.00927>. arXiv:2206.00927 [cs].
- Ma, X., Fang, G., Mi, M. B., and Wang, X. Learning-to-Cache: Accelerating Diffusion Transformer via Layer Caching, November 2024. URL <http://arxiv.org/abs/2406.01733>. arXiv:2406.01733 [cs].
- Ma, Y., Du, L., Wei, L., Chen, K., Xu, Q., Wang, K., Feng, G., Lu, G., Liu, L., Qi, X., Zhang, X., Tao, Z., Feng, H., Jiang, Z., Xu, Y., Huang, Z., Zhuang, Y., Xu, H., Hu, J., Lan, Z., Zhao, J., Li, J., and Zheng, D. dinfer: An efficient inference framework for diffusion language models. *arXiv preprint arXiv: 2510.08666*, 2025.
- Meshchaninov, V., Chimbulatov, E., Shabalin, A., Abramov, A., and Vetrov, D. Compressed and Smooth Latent Space for Text Diffusion Modeling, June 2025. URL <http://arxiv.org/abs/2506.21170>. arXiv:2506.21170 [cs].
- Ni, J., Liu, Q., Dou, L., Du, C., Wang, Z., Yan, H., Pang, T., and Shieh, M. Q. Diffusion Language Models are Super Data Learners, November 2025. URL <http://arxiv.org/abs/2511.03276>. arXiv:2511.03276 [cs].
- Nie, S., Zhu, F., Du, C., Pang, T., Liu, Q., Zeng, G., Lin, M., and Li, C. Scaling up Masked Diffusion Models on Text, February 2025a. URL <http://arxiv.org/abs/2410.18514>. arXiv:2410.18514 [cs].
- Nie, S., Zhu, F., You, Z., Zhang, X., Ou, J., Hu, J., Zhou, J., Lin, Y., Wen, J.-R., and Li, C. Large Language Diffusion Models, February 2025b. URL <http://arxiv.org/abs/2502.09992>. arXiv:2502.09992 [cs].
- NVIDIA. NVIDIA TensorRT-LLM Documentation. <https://docs.nvidia.com/tensorrt-llm/index.html>, January 2026. Accessed: 2026-01-28.
- Pan, Z., Liu, J., He, H., Cai, J., and Zhuang, B. Stitched ViTs are Flexible Vision Backbones, November 2023. URL <http://arxiv.org/abs/2307.00154>. arXiv:2307.00154 [cs].
- Pan, Z., Zhuang, B., Huang, D.-A., Nie, W., Yu, Z., Xiao, C., Cai, J., and Anandkumar, A. T-Stitch: Accelerating Sampling in Pre-Trained Diffusion Models with Trajectory Stitching, February 2024. URL <http://arxiv.org/abs/2402.14167>. arXiv:2402.14167 [cs].
- Peebles, W. and Xie, S. Scalable Diffusion Models with Transformers, March 2023. URL <http://arxiv.org/abs/2212.09748>. arXiv:2212.09748 [cs].
- Rombach, R., Blattmann, A., Lorenz, D., Esser, P., and Ommer, B. High-Resolution Image Synthesis with Latent Diffusion Models, April 2022. URL <http://arxiv.org/abs/2112.10752>. arXiv:2112.10752 [cs].
- Rütte, D. v., Fluri, J., Pooladzandi, O., Schölkopf, B., Hofmann, T., and Orvieto, A. Scaling Behavior of Discrete Diffusion Language Models, December 2025. URL <http://arxiv.org/abs/2512.10858>. arXiv:2512.10858 [cs].
- Sahoo, S. S., Arriola, M., Schiff, Y., Gokaslan, A., Marroquin, E., Chiu, J. T., Rush, A., and Kuleshov, V. Simple and Effective Masked Diffusion Language Models, November 2024. URL <http://arxiv.org/abs/2406.07524>. arXiv:2406.07524 [cs].
- Sahoo, S. S., Yang, Z., Akhauri, Y., Liu, J., Singh, D., Cheng, Z., Liu, Z., Xing, E., Thickestun, J., and Vahdat, A. Esoteric Language Models, June 2025. URL <http://arxiv.org/abs/2506.01928>. arXiv:2506.01928 [cs].
- Salimans, T. and Ho, J. Progressive Distillation for Fast Sampling of Diffusion Models, June 2022. URL <http://arxiv.org/abs/2202.00512>. arXiv:2202.00512 [cs].
- Shabalin, A., Meshchaninov, V., and Vetrov, D. Smoothie: Smoothing Diffusion on Token Embeddings for Text Generation, May 2025. URL <http://arxiv.org/abs/2505.18853>. arXiv:2505.18853 [cs] version: 1.
- Shen, M., Chen, P., Ye, P., Xia, G., Chen, T., Bouganis, C.-S., and Zhao, Y. MD-DiT: Step-aware Mixture-of-Depths for Efficient Diffusion Transformers. November 2024. URL [https://openreview.net/forum?id=1jWhiakK7N&referrer=%5Bthe%20profile%20of%20Guoxuan%20Xia%5D\(%2Fprofile%3Fid%3D~Guoxuan\\_Xia1\)](https://openreview.net/forum?id=1jWhiakK7N&referrer=%5Bthe%20profile%20of%20Guoxuan%20Xia%5D(%2Fprofile%3Fid%3D~Guoxuan_Xia1)).
- Shi, J., Han, K., Wang, Z., Doucet, A., and Titsias, M. K. Simplified and Generalized Masked Diffusion for Discrete Data, January 2025. URL <http://arxiv.org/abs/2406.04329>. arXiv:2406.04329 [cs].
- Song, J., Meng, C., and Ermon, S. Denoising Diffusion Implicit Models, October 2022. URL <http://arxiv.org/abs/2010.02502>. arXiv:2010.02502 [cs].
- Song, Y., Sohl-Dickstein, J., Kingma, D. P., Kumar, A., Ermon, S., and Poole, B. Score-Based Generative Modeling through Stochastic Differential Equations, February 2021. URL <http://arxiv.org/abs/2011.13456>. arXiv:2011.13456 [cs].

- Song, Y., Dhariwal, P., Chen, M., and Sutskever, I. Consistency Models, May 2023. URL <http://arxiv.org/abs/2303.01469>. arXiv:2303.01469 [cs].
- Tang, S., Wang, Y., Ding, C., Liang, Y., Li, Y., and Xu, D. AdaDiff: Accelerating Diffusion Models through Step-Wise Adaptive Computation, August 2024. URL <http://arxiv.org/abs/2309.17074>. arXiv:2309.17074 [cs].
- Touvron, H., Martin, L., Stone, K., Albert, P., Almahairi, A., Babaei, Y., Bashlykov, N., Batra, S., Bhargava, P., Bhosale, S., Bikel, D., Blecher, L., Ferrer, C. C., Chen, M., Cucurull, G., Esiobu, D., Fernandes, J., Fu, J., Fu, W., Fuller, B., Gao, C., Goswami, V., Goyal, N., Hartshorn, A., Hosseini, S., Hou, R., Inan, H., Kardas, M., Kerkez, V., Khabsa, M., Kloumann, I., Korenev, A., Koura, P. S., Lachaux, M.-A., Lavril, T., Lee, J., Liskovich, D., Lu, Y., Mao, Y., Martinet, X., Mihaylov, T., Mishra, P., Molybog, I., Nie, Y., Poulton, A., Reizenstein, J., Rungta, R., Saladi, K., Schelten, A., Silva, R., Smith, E. M., Subramanian, R., Tan, X. E., Tang, B., Taylor, R., Williams, A., Kuan, J. X., Xu, P., Yan, Z., Zarov, I., Zhang, Y., Fan, A., Kambadur, M., Narang, S., Rodriguez, A., Stojnic, R., Edunov, S., and Scialom, T. Llama 2: Open foundation and fine-tuned chat models. *arXiv preprint arXiv: 2307.09288*, 2023.
- Vaswani, A., Shazeer, N., Parmar, N., Uszkoreit, J., Jones, L., Gomez, A. N., Kaiser, L., and Polosukhin, I. Attention is all you need. *arXiv preprint arXiv: 1706.03762*, 2017.
- Wang, G., Schiff, Y., Sahoo, S. S., and Kuleshov, V. Re-masking Discrete Diffusion Models with Inference-Time Scaling, May 2025. URL <http://arxiv.org/abs/2503.00307>. arXiv:2503.00307 [cs].
- Wu, C., Zhang, H., Xue, S., Diao, S., Fu, Y., Liu, Z., Molchanov, P., Luo, P., Han, S., and Xie, E. Fast-dLLM v2: Efficient Block-Diffusion LLM, September 2025a. URL <http://arxiv.org/abs/2509.26328>. arXiv:2509.26328 [cs].
- Wu, C., Zhang, H., Xue, S., Liu, Z., Diao, S., Zhu, L., Luo, P., Han, S., and Xie, E. Fast-dLLM: Training-free Acceleration of Diffusion LLM by Enabling KV Cache and Parallel Decoding, July 2025b. URL <http://arxiv.org/abs/2505.22618>. arXiv:2505.22618 [cs].
- Yang, A., Li, A., Yang, B., Zhang, B., Hui, B., Zheng, B., Yu, B., Gao, C., Huang, C., Lv, C., Zheng, C., Liu, D., Zhou, F., Huang, F., Hu, F., Ge, H., Wei, H., Lin, H., Tang, J., Yang, J., Tu, J., Zhang, J., Yang, J., Yang, J., Zhou, J., Zhou, J., Lin, J., Dang, K., Bao, K., Yang, K., Yu, L., Deng, L., Li, M., Xue, M., Li, M., Zhang, P., Wang, P., Zhu, Q., Men, R., Gao, R., Liu, S., Luo, S., Li, T., Tang, T., Yin, W., Ren, X., Wang, X., Zhang, X., Ren, X., Fan, Y., Su, Y., Zhang, Y., Zhang, Y., Wan, Y., Liu, Y., Wang, Z., Cui, Z., Zhang, Z., Zhou, Z., and Qiu, Z. Qwen3 technical report. *arXiv preprint arXiv: 2505.09388*, 2025.
- Yang, C. and Holtzman, A. LLM Probability Concentration: How Alignment Shrinks the Generative Horizon, October 2025. URL <http://arxiv.org/abs/2506.17871>. arXiv:2506.17871 [cs] version: 2.
- Yang, S., Chen, Y., Wang, L., Liu, S., and Chen, Y. DE-NOISING DIFFUSION STEP-AWARE MODELS. 2024.
- Ye, J., Xie, Z., Zheng, L., Gao, J., Wu, Z., Jiang, X., Li, Z., and Kong, L. Dream 7B: Diffusion Large Language Models, August 2025a. URL <http://arxiv.org/abs/2508.15487>. arXiv:2508.15487 [cs].
- Ye, Z., Chen, L., Lai, R., Lin, W., Zhang, Y., Wang, S., Chen, T., Kasikci, B., Grover, V., Krishnamurthy, A., and Ceze, L. Flashinfer: Efficient and customizable attention engine for llm inference serving. *arXiv preprint arXiv: 2501.01005*, 2025b.
- Zhao, W., Han, Y., Tang, J., Wang, K., Luo, H., Song, Y., Huang, G., Wang, F., and You, Y. DyDiT++: Dynamic Diffusion Transformers for Efficient Visual Generation, April 2025. URL <http://arxiv.org/abs/2504.06803>. arXiv:2504.06803 [cs].
- Zur, A., Geiger, A., Lubana, E. S., and Bigelow, E. Are language models aware of the road not taken? Token-level uncertainty and hidden state dynamics, November 2025. URL <http://arxiv.org/abs/2511.04527>. arXiv:2511.04527 [cs] version: 1.

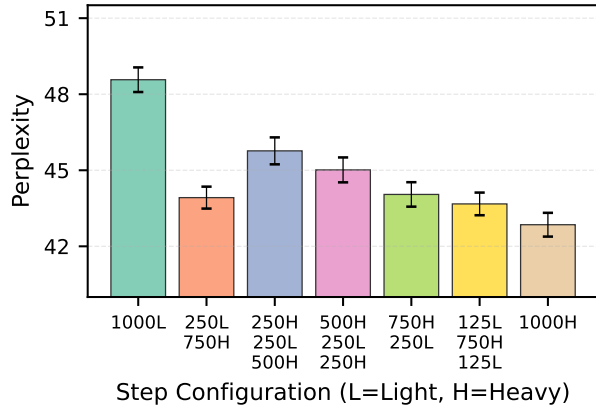


Figure 8. Generative perplexity (GPT-2) for hand-crafted model schedules using a heavy 12-block model and a light 6-block model with exactly 250/1000 light steps. Each bar label encodes a schedule as contiguous segments, e.g., (L125, H750, L125) denotes the sandwich schedule (125 light steps, 750 heavy steps, 125 light steps)

### A. Additional Models

Additional hand-crafted schedules for light models with 6,8 and 10 blocks are presented in Figures 8,10 and 11 and exhibit the same qualitative pattern.

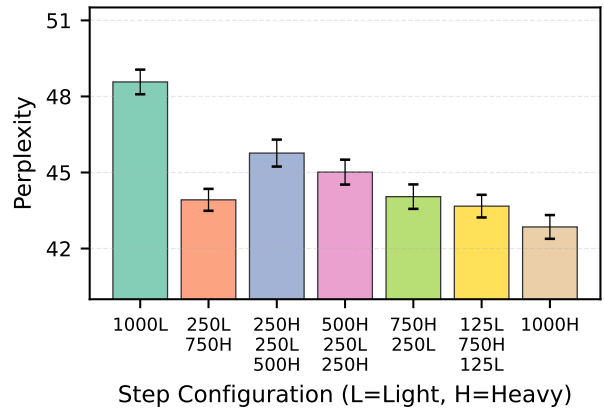


Figure 9. Generative perplexity (GPT-2) for hand-crafted model schedules using a heavy 12-block model and a light 6-block model with exactly 250/1000 light steps. Each bar label encodes a schedule as contiguous segments, e.g., (L125, H750, L125) denotes the sandwich schedule (125 light steps, 750 heavy steps, 125 light steps)

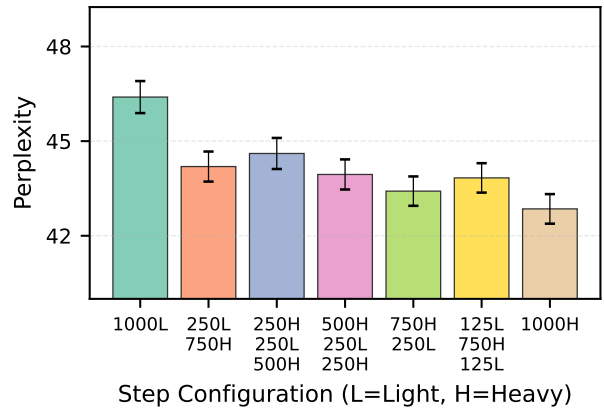


Figure 10. Generative perplexity (GPT-2) for hand-crafted model schedules using a heavy 12-block model and a light 8-block model with exactly 250/1000 light steps. Each bar label encodes a schedule as contiguous segments, e.g., (L125, H750, L125) denotes the sandwich schedule (125 light steps, 750 heavy steps, 125 light steps)

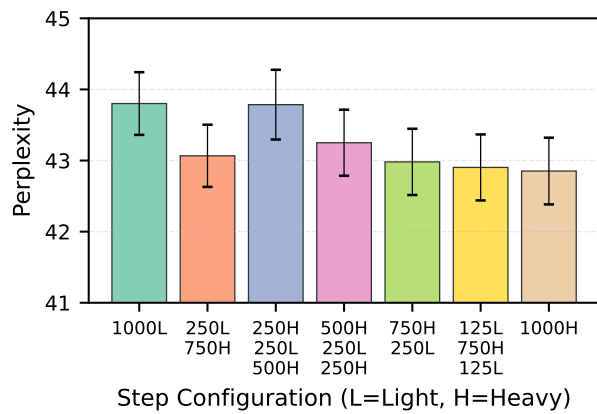


Figure 11. Generative perplexity (GPT-2) for hand-crafted model schedules using a heavy 12-block model and a light 10-block model with exactly 250/1000 light steps. Each bar label encodes a schedule as contiguous segments, e.g., (L125, H750, L125) denotes the *sandwich* schedule (125 light steps, 750 heavy steps, 125 light steps)